The web of three–planet resonances in the Outer Solar System. *

Massimiliano Guzzo
Università degli Studi di Padova
Dipartimento di Matematica Pura ed Applicata,
via Belzoni 7, 35131 Padova, Italy.
E–mail address: guzzo@math.unipd.it

Abstract

In this paper we numerically detect the web of three–planet resonances (i.e. resonances among mean anomalies, nodes and perihelia of three planets) with respect to the variation of the semi–major axis of Saturn and Jupiter, in a model including the planets from Jupiter to Neptune. The measure confirms the relevance of these resonances in the long–term evolution of the outer Solar System and provides a technique to identify some of the related coefficients.

Key Words: Planetary Dynamics; Jovian Planets; Resonances, Celestial Mechanics.

1 Introduction

The problem of the stability of our Solar System is one of the main problems of Celestial Mechanics. In the last decades this problem has been studied by means of long–term numerical integrations (Sussman and Wisdom 1988; Laskar 1989; Nobili et al. 1989; Sussman and Wisdom 1992; Laskar 1996) which demonstrated that while the system does not show significant instabilities (especially for the outer planets), it is nevertheless chaotic. Laskar (1990) found secular resonances responsible for the chaos of the inner planets. The chaotic nature of the outer planets is instead a problem which is still under study, with a recent advancement on its comprehension made by Murray and Holman (1999). Sussmann and Wisdom (1992) remarked that long–term integrations of the outer Solar System made with different integrators and different integration steps agreed that the system is chaotic, but gave substantially different Lyapunov times. They conjectured that these discrepancies could be due to a high sensitivity of the dynamics of the system on the initial conditions, so that little changes in the integration scheme could potentially give different results. Murray and Holman (1999) found that the chaotic nature of the solutions is very sensitive to small changes of the semi–major axis of Uranus, and identified the three–body resonances among Jupiter, Saturn and Uranus as the main responsible for this. They also provided a heuristic model to show that these resonances can produce chaotic diffusion of the planets on very long times.

Three–body resonances have been already used to explain in great detail the dynamical structure of the asteroid belt (Murray, Holman and Potter 1998, Nesvorny and Morbidelli 1998a, Nesvorny and Morbidelli 1998b, Morbidelli and Nesvorny 1999). In particular, they allow one to explain much of the slow chaos arising at moderate eccentricities.

The importance of three–body resonances for the dynamics is due to the fact that though they are

*This is the author's version of a work that was accepted for publication in Icarus. Changes resulting from the publishing process, such as peer review, editing corrections, structural formatting, and other quality control mechanisms, may not be reflected in this document. Changes may have been made to this work since it was submitted for publication. A definitive version was subsequently published in ICARUS, Volume 174, Issue 1, March 2005, Pages 273-284. DOI: http://dx.doi.org/10.1016/j.icarus.2004.10.015.

second order resonances with respect to the planetary masses (they include at least three objects), and therefore their amplitude is small, they are nevertheless organized in multiplets that typically can overlap (Nesvorny and Morbidelli 1998b) at moderate eccentricities, giving rise to chaotic motion and possibly to chaotic diffusion (for asteroids, diffusion times can be typically 100Myr). In the planetary case, the structure of the multiplets is the following. Denoting by $a_j, e_j, i_j, \lambda_j, \omega_j, \Omega_j$ the orbital elements of the j–th planet, with j running from 5 (Jupiter) to 8 (Neptune), a three–body resonance occurs when there exist three integers n_i, n_j, n_k such that:

$$n_i \dot{\lambda}_i + n_j \dot{\lambda}_j + n_k \dot{\lambda}_k \sim 0 \quad , \tag{1}$$

more precisely when this quantity is of the same order of the secular frequencies $\dot{\omega}_h, \dot{\Omega}_h$ $(h = 5, \dots, 8)$.

Therefore, as explained in Murray an Holman 1999, in the phase space of the planets there are initial conditions such that for some integer values of the k_h, k'_h the angle:

$$n_i \lambda_i + n_j \lambda_j + n_k \lambda_k + \sum_{h=5}^{8} (k_h \omega_h + k'_h \Omega_h) \tag{2}$$

is resonant, i.e. it is librating, or it is in a regime of chaotic alternation of librations and circulations. Because the secular frequencies $\dot{\omega}_h$, $\dot{\Omega}_h$ are of the same order of the planetary masses $m_5, \dots, m_8$ (the mass of the Sun is 1; hereafter for convenience we denote also $\epsilon = m_5$), while the main contribution to the frequencies $\dot{\lambda}_i$ is given by the Keplerian approximation, for any fixed (n_i, n_j, n_k) all possible values of the k_h, k'_h generate a multiplet of resonances (2) separated in semi-major axis by order ϵ. But the strength of resonant harmonics is of order ϵ^2 (see Nesvorny and Morbidelli 1998b; Murray and Holman 1999, and also section 4) so that their amplitude in semi–major axis is of order ϵ. Therefore, because the distances among these resonances and their amplitudes are of the same order, they can overlap.

To determine analytically the overlapping of these resonances is a complicated technical problem. In the case of a planar approximation of the asteroid motion an analytic approach for the precise computation of the location and separation of the different components of the multiplet has been done in Nesvorny and Morbidelli 1998b. Numerical approaches have been also used to detect the location and the structure of the resonances (Morbidelli and Nesvorny 1999), based on the computation of the largest Lyapunov exponent of the system (actually, a Fast Lyapunov Indicator, see Froeschlé et al. 1997) with respect to the change of a critical initial condition, and then trying to associate to the peaks of positive Lyapunov exponent a linear combination of the frequencies.

In the case of the planets, the one–dimensional spans of the parameters space provided in Murray and Holman 1999 allow one to appreciate alternation of intervals of regular motions and intervals of chaotic motions, thus excluding a uniform covering of the phase space by resonance overlapping.

Moreover, two dimensional spans of the parameters space allow one to appreciate the geometry of the resonances. In particular they allow one to appreciate if the resonances constitute a regular web (the so called Arnold web, see Froeschlé et al. 2000) or instead there are some local overlappings. These two scenarios can have different implications on the long–term stability of the system (see Morbidelli and Guzzo 1997, Guzzo and Morbidelli 1997, Morbidelli 2002).

Mitchenko and Ferraz–Mello (2001a) provide two–dimensional explorations of the phase–space around each planet obtained by changing the semi–major axis and the eccentricity of one planet in each exploration. The results, obtained with 3 Myr numerical integrations, confirm that within a distance of order 10^{-2} au from our Solar System there are some important three–planet resonances. Nevertheless, due to the limited integration time they cannot detect the three–planet resonances described by Murray and Holman (1999).

In this article, using a numerical approach based on the combined use of the fast Lyapunov indicator method (FLI hereafter) and of frequency analysis (Laskar 1993) we will provide a direct representation of the three–planet resonances on a two–dimensional grid of initial conditions which is obtained changing the values of the initial semi–major axis of Jupiter and Saturn.

As we explain in section 2, these are expected to be critical parameters for the exploration of the three–planet resonances in a neighborhood of the true initial condition of our Solar System.

The present exploration concerns a very small neighbourhood of the true solar system, (from $2 \cdot 10^{-5}$ to $4 \cdot 10^{-3}$ au) and the integration time is 20 Myr for each initial condition, so that we can detect the weak three–planet resonances which were indicated by Murray and Holman (1999) as the origin of the chaos of the outer planets.

Our results establish that in this small neighborhood of the true Solar System (obtained from JPL DE405) some families of three planet–resonances constitute an intricate web. The typical separation of these resonances is of order 10^{-5} rad/yr, and therefore a change in the semi–major axis of Jupiter (or Saturn) of about 10^{-5} au can change the dynamical state of the system. The results agree with those of Murray and Holman 1999, who find the family of resonances $(n_5, n_6, n_7) \sim (3, -5, -7)$, but also we find other families of three–body resonances associated to the coefficients $n_6/n_5 = 3$, $11/4 \sim 2.73$, 1, 4, $17/6 \sim 2.84$, 6 (see section 3). It is relevant that all these families are consistent with the small denominators found by Bretagnon (Bretagnon 1981, 1982) in his analysis of the solution of the Solar System at third order in planetary masses. In Bretagnon papers the question about the location of the resonances associated to these small divisors (nor its arrangment in phase space as a web) is not raised. Nevertheless the appearence of these small denominators in the analytic solution suggests that they should be in some sense relevant to the dynamics of the Solar System, as it is precisely shown in this paper.

The position of the true Solar System with respect to the web of three–planet resonances is a peculiar one. In fact, the true Solar System is at the edge of a crossing of these resonances, and therefore its dynamical state is particularly sensitive to very small changes of the initial conditions. The computation of the Lyapunov exponent exhibits the puzzling dependence on the integration step and on the initial conditions which was first described by Sussman and Wisdom 1992. This can be possibly due to intermittency phenomena, which usually characterize the border of resonance crossings. This aspect will be investigated in a forthcoming paper.

As a final comment, we spend a few words about the geometry of three–planet resonances, which, as it will be shown in figure 2, resembles the celebrated Arnold web. Indeed, the web of figure 2 is qualitatively similar to the one numerically detected for a three degrees of freedom system (Froeschlé et al. 2000), except for the resolution of the figure which, for the Solar System, is necessary limited by CPU cost. This gives indication that an eventual diffusion in semi–major axis space should be a very slow Arnold diffusion along the three–planet resonances, as it is suggested by a preliminary numerical test (see section 4.2). However, our results do not predict the geometry of resonances for the other degrees of freedom, expecially those related to eccentricities and inclinations of the planets.

This article is organized as follows: section 2 is devoted to a preliminary numerical exploration of the Sun–Jupiter–Saturn system; in section 3 we describe the web of three–planet resonances in the small neighbourhood of our Solar System; section 4 is devoted to the analysis of a test orbit in a three–planet resonance. Section 5 is devoted to the description of the numerical methods used in the paper.

2 The 5-2 mean motion resonance

Before discussing the full model which includes the four giant planets, we find instructive to show the results for the restricted systems Sun–Jupiter–Saturn (for a detailed investigation of the problem see Michtchenko and Ferraz–Mello 2001b) and Sun–Jupiter–Saturn–Uranus.

As is well known since Laplace, the motion of Saturn and Jupiter is affected by the quasi–resonance 5-2, i.e. $2\dot{\lambda}_5 - 5\dot{\lambda}_6 \sim 0$. Actually, the system is not in the resonance, because on average the critical angle $2\lambda_5 - 5\lambda_6$ advances monotonically with respect to time, but the vicinity of the 5–2 resonance forces large oscillations of it. To appreciate the relative position of the Sun–Jupiter–Saturn system with respect to the 5–2 resonance we represent numerically the web of resonances of the system using the FLI indicator (Froeschlé et al. 1997). Other two–dimensional representations of the resonances of the Solar System, showing in particular the location of the Solar System with respect to the 5–2 resonance, can be found in Robutel and Laskar 2001, Michtchenko and Ferraz–Mello 2001a, Laskar 2003, Robutel 2004.

The computation of the FLI on a grid of initial conditions allows us to display a clear picture of the web of resonances of the system. As it is well known, in the parameters space of a complicated dynamical system (such as the one which represents the evolution of the planets) there is a complicated distribution of regular motions and chaotic motions. Of course, regular motions are stable. Instead, it is the distribution of chaotic orbits which provides insights on the long–term stability of the system. For example, if the chaotic motions are organized in a regular web (the so–called Arnold web) then there is a strong chance that even chaotic motions are practically stable over very long times. Instead, if the distribution of the chaotic orbits does not constitutes a regular web and looks like a chaotic see, then there is the possibility of Chirikov diffusion. These different situations can be discriminated by computing a dynamical indicator on a grid of initial conditions.

The FLI indicator is the logarithm of the norm of a tangent vector $v(t)$ (computed with the variational equations of the dynamics) taken at the end of the computation, with the same initial tangent vector $v(0)$ for any initial condition on the grid. As is well known, the growth of tangent vectors is linear in time in the case of regular orbits, while it is exponential in time in the case of chaotic orbits. To compute the largest Lyapunov exponent λ it is necessary to compute the growth of tangent vectors for times t which are sufficiently long so that the quantity $\log|v(t)|/t$ converges to λ. However, in order to discriminate between regular and chaotic orbits it is sufficient to compute $|v(t)|$ for such a (small) time such that the exponential growth law can be distinguished from the linear growth law (Froeschlé et al. 1997). Therefore, computing the FLI on a grid of initial conditions allows one to discriminate between the resonant chaotic motions and the regular motions because the formers take the higher FLI values. A more subtle point is that the FLI allows one also to discriminate between the regular orbits which are inside a resonance (such as librating motions) and the regular orbits which are outside a resonance (Froeschlé et al 2000; Guzzo et al. 2002). In fact, the FLI of regular motions inside a resonance is lower than the FLI of regular motions which are outside the resonance.

Summarizing these facts, when computing the FLI on a grid of initial conditions, the resonances are well individuated as the regions with the higher and the lower FLI values, while the uniform intermediate value characterizes the regular non resonant motions. Therefore, in each picture of figures 1 and 2 the yellow and the dark lines identify the resonances, while the uniform background color identifies regular non resonant motions. For the detailed explanation of the FLI and its use in the detection of the geometry of resonances of a system we refer to Froeschlé et al. 2000, and to Guzzo et al. 2002.

Coming back to the planetary problem, figure 1 top–left (see section 5 for the explanation of the integrated model and for the choice of initial conditions) reports the computation of the FLI for the Sun–Jupiter–Saturn system on a two dimensional grid of initial conditions, obtained keeping constant all initial values of the orbital elements of the two planets, except the initial values of their semi–major axes. This choice was motivated by the fact that semi–major axes are the elements which mainly determine the mean motion resonances. From this picture it is clear that the system is *near* the 5–2 resonance, but *not in* it: the 5-2 resonance is clearly identified as the yellow band of chaotic motions, while the initial condition of the 'true' Solar System[1] is definitely outside this chaotic band, and it is in a region of regular motions (characterized in the picture by the orange value of the FLI).

This experimental fact implies that the mean anomalies of the two planets can be effectively averaged out from the equations of motion of the system, which can be therefore described by its secular equations. Then, an analytic study of the secular system can be done as in Locatelli and Giorgilli 2000, who proved with computer assisted methods that the Sun–Jupiter–Saturn secular system has plenty of KAM tori near the true initial condition, providing perpetual stability. On figure 1 top–right we report also an exploration of the initial conditions very near the true Sun–Jupiter system: the uniform color confirms that no relevant resonances can be found nearby the true Sun–Jupiter–Saturn

[1] As explained in section 5, by 'true' Solar System we refer to the ephemerids of the outer Solar System as provided by the DE405 digital ephemerids, with a barycentric correction due to the presence of the inner planets (see Milani and Knežević 1992). This can be considered as one of the most precise initial conditions which we can use, but possible errors in DE405 and in the numerical integrations force us to consider the true system in a small neighborhood of this initial condition.

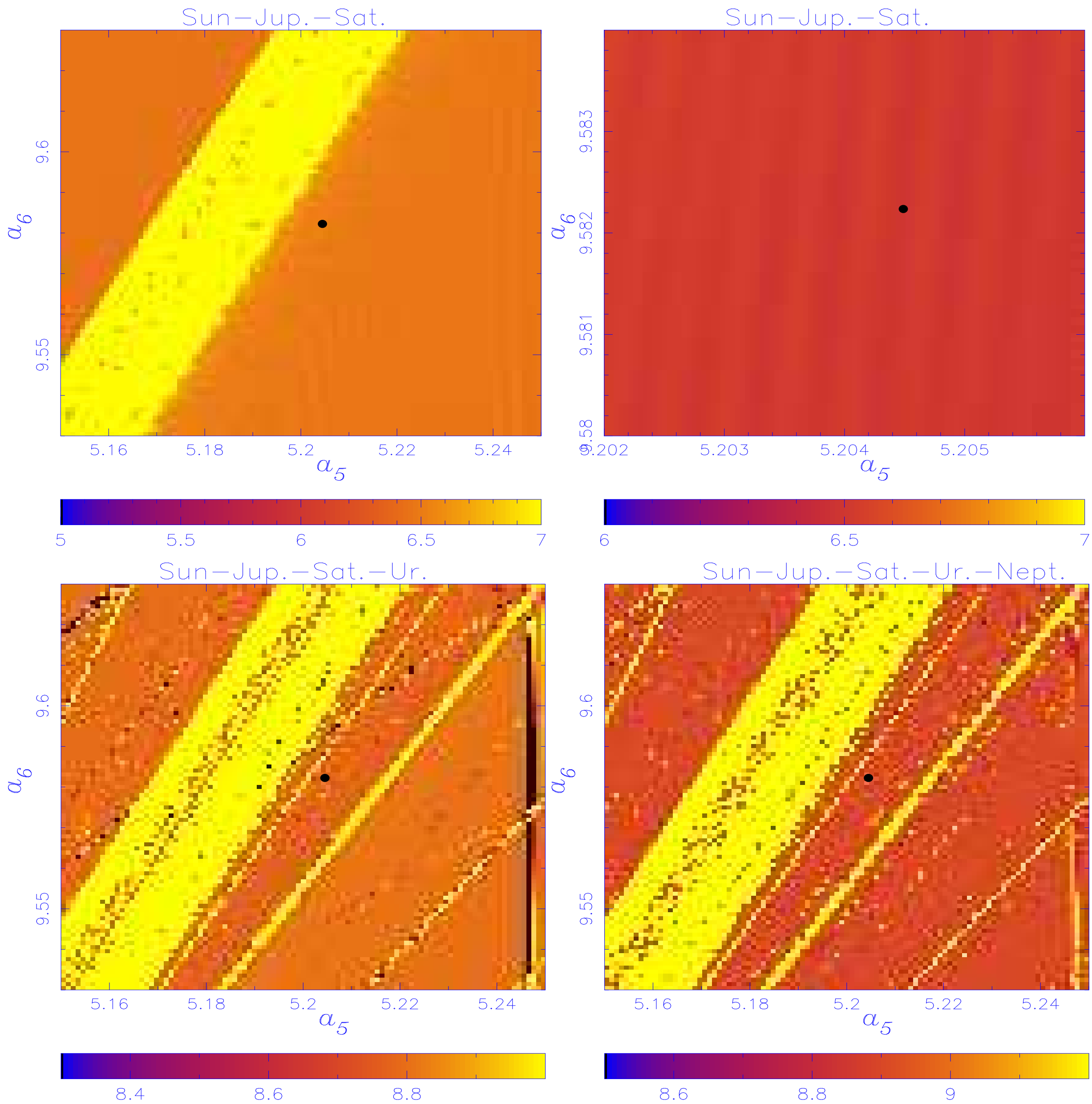

Figure 1: The four panels report on a color scale the FLI associated to each initial condition on a two–dimensional grid, obtained by changing the semi–major axis of Jupiter and Saturn a_5, a_6. The lines defined by the higher value of the FLI (yellow in the color scale) or the lower value of the FLI (dark orange in the color scale) correspond to resonances. The uniform background color correspond to regular motions such as KAM tori. The integration time is 1 Myr for all integrations. The 'true' initial condition of the system is represented by a black dot. **Top left:** FLI of the Sun–Jupiter–Saturn system; the 5–2 resonance is clearly identified as the large yellow band. The 'true' Solar System is outside the resonance. **Top right:** Enlargement of the previous picture around the 'true' initial condition. The FLI does not reveal any structure. **Bottom left:** FLI of the Sun–Jupiter–Saturn–Uranus system. The geometry of resonances has drastically changed with respect to the Sun–Jupiter–Saturn system: many other resonances, different from the 5–2, have appeared, and they correspond to three–body resonances with Uranus. The 'true' system is very near on of these resonances, so a more detailed study around it is necessary. **Bottom right:** FLI of the Sun–Jupiter–Saturn–Uranus–Neptune system. The picture is similar to the previous one, with the exception of some more small resonances.

system.

We now include in the system also Uranus and Neptune. These two planets introduce of course new resonances. This can be seen in figure 1 bottom–right, where we repeated the computations of figure 1 top–left, but for the four planets model: new important resonances appear. Beside the most important 5–2 resonance, many other resonances constitute a web in the parameter space, and all these new resonances are related to the orbital elements of Jupiter, Saturn, and at least one planet among Uranus and Neptune. The picture is drastically changed with respect to the Sun–Jupiter–Saturn case, and the appearance of the web of second order resonances forces a more accurate study of the neighbourhood of the true initial condition. In figure 1 bottom–left we report also the same computation done on the Sun–Jupiter–Saturn–Uranus–Neptune system. The picture is very similar to the previous one, except for the lack of few resonances related to Neptune.

3 The web of three–planet resonances

Motivated by the results of the previous section, we explored a very small window of the parameters space around the initial condition corresponding to the true initial condition of the Sun–Jupiter–Saturn–Uranus–Neptune system. As explained in Murray and Holman 1999, three–body resonances are expected to be produced by the mixing of the 5-2 quasi–mean motion resonance with other possible quasi mean motion resonances. Therefore, Murray and Holman explored a one–dimensional grid of initial conditions obtained changing only the semi–major axis of Uranus. Here, we do a different choice exploring a two dimensional grid of initial conditions obtained by changing the semi–major axes of Jupiter and Saturn[2], therefore changing the relative position of Jupiter–Saturn with respect to the 5–2 resonance, which enters in many three–body resonances. Moreover, profiting of the study of Murray and Holman who predicted typical periods for these resonances of about 10 Myr, we integrated the system up to 20 Myr. This integration time is sufficient for the FLI to evidenciate resonances with libration periods of this order. The results are shown in Figure 2. There is a technical difference between the bottom panel of figure 2 and the ones on the top, because the x, y axes do not report the semi–major axes a_5, a_6, but the frequencies $\dot\lambda_5, \dot\lambda_6$, obtained with a frequency analysis of the solution in the time interval $t \in [0, 10^4]yr$. Of course, if one computes the frequencies on different times intervals $t \in [t_0, t_0 + 10^4]yr$ one obtains different values. However, because the main variation of the computed frequencies with respect to the initial time t_0 is a quasi–periodic oscillation, for the purpose of using these values to represent the geometry of resonances it is sufficient to keep the same $t_0 = 0$ for all initial conditions of the grid.

The correspondence between the semi–major axes and the frequencies of the mean anomalies is the following: in addition to the two body keplerian frequencies there is a contribution due to the mutual interactions among the planets. This contribution has the effect to transform the square grid in the semi–major axes space (top panels of figure 2) to the parallelogram picture in the frequency space which can be seen in the bottom panel of figure 2 (because the frequency of Saturn is affected by the interaction with Jupiter more than the frequency of Jupiter is affected by the interaction with Saturn).

The representation of the FLI indicator with respect to a two dimensional grid of frequencies allows us to identify, for each resonant multiplet associated to $n_5\lambda_5 + n_6\lambda_6 + n_j\lambda_j$, with some $j = 7, 8$, the ratio n_6/n_5, which is the slope of the resonant line in the two–dimensional figure.

In fact, any linear combination of $n_5\lambda_5 + n_6\lambda_6 + n_j\lambda_j$ with the secular angles can produce a three–planet resonance which appears as a straight line in the space of frequencies $\dot\lambda_5, \dot\lambda_6$. The multiplet associated to fixed n_5, n_6, n_j is represented in such a plane by a family of parallel lines.

Following this technique, it is possible to identify the presence of multiplets associated to the ratios: $2.735 \sim 11/4$ (family of yellow lines on the bottom–right); 3 (main yellow line in the middle); $1.67 \sim 5/3$; $2.84 \sim 17/6$ (small yellow resonances on the top–left); 6.0, 4.0 and 1. In the picture one can also appreciate some horizontal resonances, which correspond to three–planet resonances which do not depend on the semi–major axis of Jupiter

[2] The grid covers a variation of the semi major axes of Jupiter and Saturn from 5.202 to 5.206 and from 9.58 to 9.584 respectively (epoch 5 June 2000) using steps of $2\ 10^{-5}$ au.

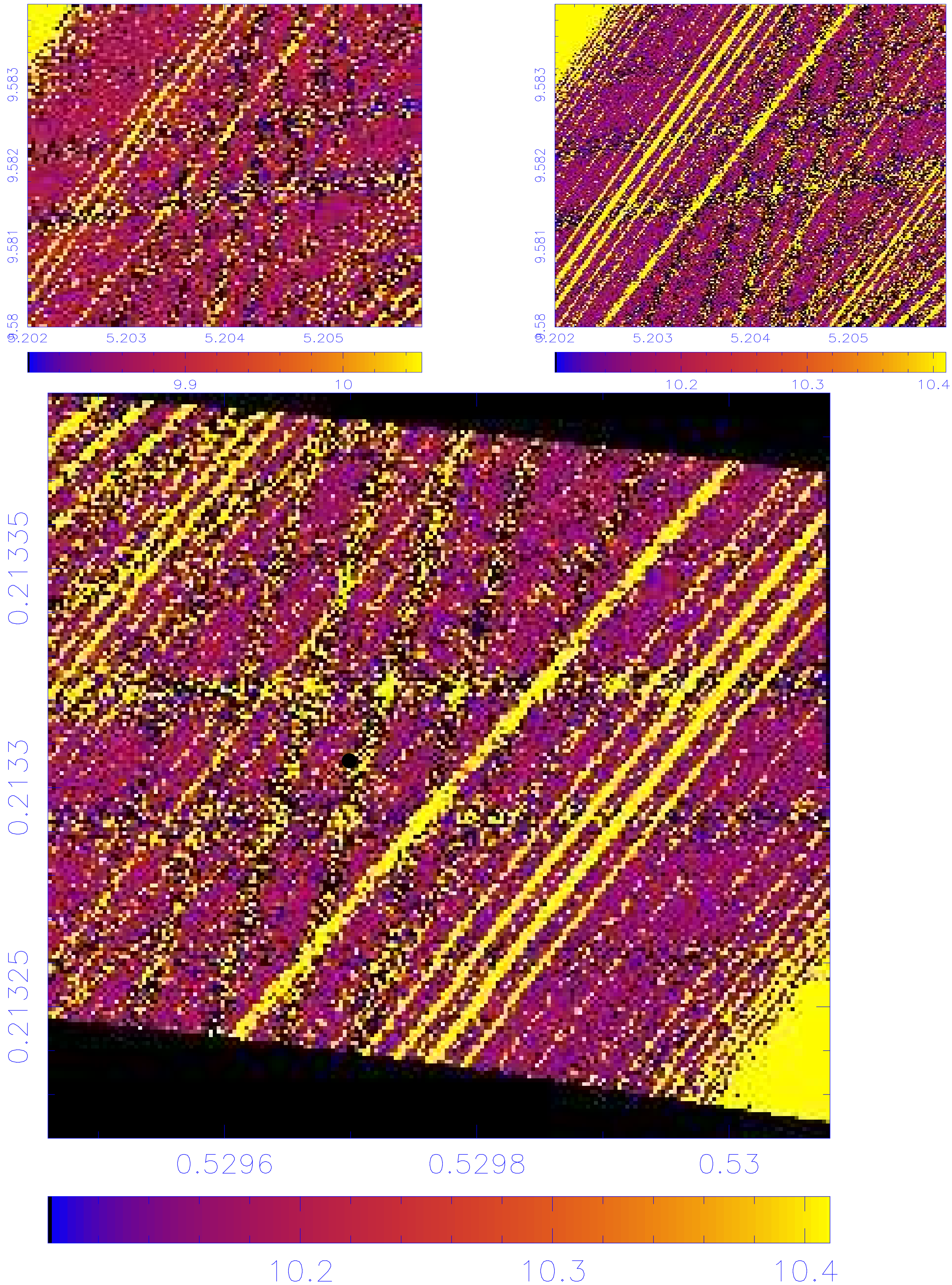

Figure 2: The panels report on a color scale the FLI associated to each initial condition on a two–dimensional grid, obtained by changing the semi–major axis of Jupiter and Saturn a_5, a_6 very near the 'true' initial condition. **Top Left:** FLI of the Sun–Jupiter–Saturn–Uranus–Neptune system; the system is integrated up to 10 Myr with a time step of 0.05 yr; the grid is 99 times 99. **Top Right:** Same system as before, but integrated up to 20 Myr with a time step of 0.2 yr; the grid is 200 times 200. **Bottom:** Same integration as top right, but on the x, y axes we do not report the value of the semi–major axis, but the value of the frequencies $\dot{\lambda}_5, \dot{\lambda}_6$ of the mean motions numerically computed with a frequency analysis on the time interval $[0, 10^4]yr$. The lines defined by the higher value of the FLI (yellow in the color scale) or the lower value of the FLI (dark orange in the color scale) correspond to resonances. The uniform background color corresponds to regular motions such as KAM tori. The 'true' Solar System is represented by a black dot.

(while they depend on the semi–major axis of Saturn). Note however that there are not vertical resonances, which means that all relevant three–planet resonances depend on the semi–major axis of Saturn. The true Solar System is very near the crossing among the families with ratio 1 and 4. A more complete representation of the three–planet resonances would be provided by additional numerical explorations of the planes related to Saturn–Uranus and Uranus—Neptune. However, due to the high CPU cost required by these computations they will be published in the future.

The resonances represented in figure 2 constitute a web with step–size of order of 10^{-5} rad/yr, or equivalently $10^{-5} \sim 10^{-4}$ au in semi–major axis (i.e. about 10^4 Km). Therefore, on the same range of 10^{-4} au, there are initial conditions with very different dynamical state, and this fact could explain the puzzling dependence of the Lyapunov exponent on the initial conditions. The extreme sensitivity of the location of the resonances on the initial conditions, the errors which affect the initial conditions of the true Solar System (DE405 have possible errors on Saturn ephemerids of 200-300 km, but possible larger errors on Uranus and Neptune ephemerids) and the errors which affect the numerical integration (with possible errors in frequencies of $10^{-8}-10^{-7}$ rad/yr, see Guzzo 2001) do not allow us to precisely identify the dynamical state of our Solar System, but allows us to understand that it is one of the possible dynamical states around the 'true' initial condition represented in the figure. In particular, the 'true' Solar System seems to be at the edge of the crossing among the resonances with ratio 1 and 4, and therefore the precise determination of its dynamical state is particularly critical. Our computations do not allow us to clearly understand if the true initial condition is indeed inside the resonance, or it is outside. The computation of the largest Lyapunov exponent on a time much longer than the 20 Myr used for figure 2 does not help to solve the problem. The evolution of the quantity $l(t) = \log|v(t)|/t$ versus time is reported in figure 3. It is evident that the orbit is not regular (confirming the long term integrations of the system which can be found in the literature), but because $l(t)$ is not convergent in the integration time we cannot identify $l(t)$ at the end of the integration as the largest Lyapunov exponent. The reason is that the system seems to alternate periods of chaotic motion (increase of $l(t)$) to periods of regular motion (decreasing of $l(t)$), as in the intermittent dynamical regimes. Effectively, intermittency could be find in the peculiar location of the true Solar System, such as the neighborhood of a crossing of two resonances, but this will be the subject of a forthcoming paper.

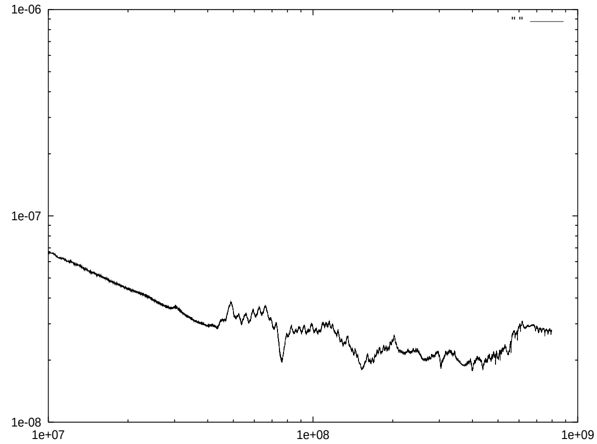

Figure 3: Computation of the largest Lyapunov exponent of the 'true' initial condition, integrated with the order four symplectic integrator described in Guzzo 2001, with small integration step of 0.01 yr. The plot reports the evolution of the quantity $\log|v(t)|/t$ versus time. The quantity $\log|v(t)|/t$ seems to behave as if the solution is chaotic. Nevertheless, the curve does not stabilizes in the integration time.

The impact of the slow chaos generated in the three–planet resonances on the long–term evolution of the Solar System is a delicate, not completely understood problem. It is clear that these resonances do not produce dramatic changes in the Solar System lifetime. Indeed, diffusion times estimated by Murray and Holman (1999) with a heuristic argument are very long (of order 10^{17} yr for Uranus's eccentricity). In order to investigate the possible impact of three–planet resonances on the diffusion in the semi–major axes space I have performed some long–term test integrations with chaotic initial conditions in the resonances. The results, which are described in section 4, suggest that indeed within Gyr timescales one can detect a drift in the direction parallel to the resonances, as it is the case of Arnold diffusion, but this kind of diffusion occurs with very small speed of order 10^{-15} au/yr.

4 Dynamics within resonances

4.1 Fourier analysis of a test orbit in the $n_6/n_5 = 3$ three planet resonance

In this section we perform a Fourier analysis of a test initial condition in one of the main three–planet resonances, i.e. the one with ratio $n_6/n_5 = 3$. Our purpose is to identify the main quasi–resonances generating the three–planet resonances, and to find a trace in the Fourier spectrum of harmonics in the range of the secular frequencies which can be related to the three–planet resonance.

We will find that the main quasi mean motion resonances are, besides the 5-2 Jupiter Saturn resonance, also the 1-3 Saturn–Uranus resonance and the 1-2 Uranus–Neptune. These quasi–resonances can be considered to be present in all the region explored, because quasi mean motion resonances are not so sensitive to the initial condition as three–body resonances. The same resonances were also individuated by Mitchenko and Ferraz Mello 2001a. It is immediate to recognize that these quasi–mean motion resonances can combine to produce all the possible three–body resonances.

We will interpret the Fourier analysis of the solution by means of Hamiltonian perturbation theory (for the detailed description of normal forms of three–body resonances in the asteroid case see Nesvorny and Morbidelli 1998b and Morbidelli 2002). This will help us to associate to each Fourier harmonic of the numerically computed solution the resonance which is responsible of it.

The Hamiltonian representation of the dynamics of the planetary problem is done using the canonical Delaunay variables $L_j, G_j, H_j, \lambda_j, \omega_j, \Omega_j$. Using standard perturbation theory (see, for example, Morbidelli 2002), one can show that the motion $L(t) - L(0)$ has the following representation:

$$L(t) - L(0) = \epsilon \sum_j \nu_j A_j(t) + \epsilon^2 k B(t) + ... \quad (3)$$

where $\nu_j \in \mathbb{Z}^4$ are the vectors related to the leading quasi resonances among two bodies, i.e. to the resonance $\nu_j^i \dot{\lambda}_i + \nu_j^k \dot{\lambda}_k \sim 0$; A_j depend quasi–periodically on time t; the integer vector $k \in \mathbb{Z}^4$ is related to the three–planet resonance $k_{i_1}\dot{\lambda}_{i_1} + k_{i_2}\dot{\lambda}_{i_2} + k_{i_3}\dot{\lambda}_{i_3} + k_{i_4}\dot{\lambda}_{i_4} \sim 0$ (one of the k_i can be 0). The above representation can be used to detect numerically the leading quasi–resonances and the leading three–planet resonances. This can be done as follows. We first compute numerically the quantity $L(t) - L(0)$ for a time span of 8.4 Myr, and then we compute the discrete Fourier transform. To increase the precision of the computation we actually compute the Fourier transform of $\phi(t)(L(t) - L(0))$, where $\phi(t)$ is the analytic window defined in Guzzo and Benettin 2001 (see Guzzo and Benettin 2001 for technical details and motivations). In such a way, we obtain a quasi–periodic representation of $\phi(t)(L(t) - L(0))$ with a discrete set of frequencies $\sigma \in \Sigma$:

$$\phi(t)(L(t) - L(0)) \sim \sum_{\sigma \in \Sigma} \nu_\sigma f_\sigma e^{i\sigma t} \quad , \quad (4)$$

with $\nu_\sigma \in \mathbb{Z}^4$. The Fourier spectrum for the test initial condition in the resonance $n_6/n_5 \sim 3$ is reported in figure 4 on the top.

The determination of the vectors ν related to the leading terms of the spectrum allows us to determine the main quasi mean motion resonances as well as the three–body resonances. In fact, denoting by

$$\sum_{\sigma \in \Sigma} F_\sigma e^{i\sigma t} \quad (5)$$

the numerically computed Fourier expansion of $\phi(t)(L(t) - L(0))$, the relevant quasi mean motion resonances correspond to the leading terms of the expansion such that $F_\sigma \in \mathbb{R}^4$ has two coefficients negligible with respect to the other two. Denoting with F_σ^i, F_σ^j the two leading coefficients, the integer vector ν_σ associated to the resonance satisfies:

$$\frac{\nu_\sigma^i}{\nu_\sigma^j} = \frac{F_\sigma^i}{F_\sigma^j} \quad (6)$$

while the other two entries are 0.

Exploring the domain of frequencies $\omega = (2\pi)/T$ up to 0.12, which corresponds to a period of about 500 yrs, we detected the following quasi mean–motion resonances:

- Jupiter–Saturn: we find a lot of periodic terms with $\nu_\sigma^6/\nu_\sigma^5 \sim 2.5$, corresponding to the leading quasi mean motion resonance $(2, -5, 0, 0)$. The largest of these terms corresponds to the frequency $\sigma \sim 6.526160 \cdot 10^{-3}$.

- Saturn–Uranus: we find a lot of periodic terms with $\nu^7_\sigma/\nu^6_\sigma \sim 3.$, corresponding to the leading quasi mean motion resonance $(0, 1, -3, 0)$. The largest of these terms corresponds to the frequency $\sigma \sim 1.080453 \cdot 10^{-2}$.

- Uranus–Neptune: we find a lot of periodic terms with $\nu^8_\sigma/\nu^7_\sigma \sim 2.$, corresponding to the leading quasi mean motion resonance $(0, 0, 1, -2)$. The largest of these terms corresponds to the frequency $\sigma \sim 1.468068 \cdot 10^{-3}$.

Then, we looked for three–planet resonances. Having chosen the initial condition in the resonance $n_6/n_5 = 3$ we expected to find many terms with $F^6_\sigma/F^5_\sigma \sim 3$. Actually, we observed many terms with ratio $F^6_\sigma/F^5_\sigma \sim 3$. Among all these terms the leading one has frequency $\sigma \sim 4.272376 \cdot 10^{-3}$ and $F^7_\sigma/F^6_\sigma \sim 0.55$, which is compatible with the combination $(2, -6, 3, 0)$, generated by $(2, -5, 0, 0)$ and $(0, -1, 3, 0)$. However, its frequency is not near the secular frequencies, so we do not expect that this is the combination generating the resonance. To find the harmonics which properly couples with the secular frequencies in order to produce a resonance we therefore look at all terms in the range of secular frequencies, i.e. we select all terms with frequency smaller than: $1.4 \cdot 10^{-4}$. The result is summarized in figure 4 on the bottom. Actually, in the frequency range up to $2 \cdot 10^{-5}$, the most relevant harmonics correspond to the ratio $F^6_\sigma/F^5_\sigma \sim 3.$, and have non–negligible components over the four planets.

4.2 Long term integration of a test orbit in the $n_6/n_5 = 3$ three planet resonance

In this subsection I describe the result of a 3 Gyr integration of a test particle in the $n_6/n_5 = 3$ three planet resonance, in order to detect eventual long–term diffusion in the semi–major axes space. From equation (3) it is evident that the projection of the motion over the semi–major axes space allows to see mainly the dominant quasi–periodic terms due to the functions $A_j(t)$. The presence of these large quasi–periodic oscillations in principle can prevent to appreciate any smaller chaotic diffusion. In order to minimize these projection effects, instead of considering the orbit $a_5(t), a_6(t)$, I consider the sequence $\tilde{a_5}(2\ k\ 10^6), \tilde{a_6}(2\ k\ 10^6)$ of the running averages of the semi–major axes in the 2 Myr intervals $t \in [2\ k\ 10^6, 2\ (k+1)\ 10^6]$. The averaged dynamics should therefore satisfy the equation: $\tilde{L}(t) - \tilde{L}(0) = \epsilon^2 k B(t) + ...$, i.e. the main contribution to the averaged dynamics is a motion parallel to the integer vector k generating the resonance (in the present case it is $k_6/k_5 = 3$). Other contributions can in principle determine a slower diffusion in the direction aligned with the resonance, i.e. an Arnold diffusion.

In figure 5 I plotted a black dot for any point of the sequence $\tilde{a_5}, \tilde{a_6}$. In figure 5a it is clear that the orbit is flattened around a segment transversal to the resonance and the the slope of the segment in the action space L_5, L_6 is precisely equal to 3.

Then we zoom in the picture in order to appreciate eany ventual Arnold diffusion in a direction parallel to the resonance. Indeed, figure 5b allows to appreciate, beyond the main motion flattened on the direction k, also a much smaller variation of the orbit of about $1.4\ 10^{-6}$ au along the direction of the resonance. This variation occurs mainly in the interval of time $[5\ 10^8, 7\ 10^8]$ yr, and therefore has an average speed of $7\ 10^{-15}$ au/yr.

5 Numerical methods

The numerical integrations reported in this paper refer to the Hamiltonian model of the Solar System, including the planets from Jupiter to Neptune (some computations shown in figure 1 include only Jupiter–Saturn, or Jupiter–Saturn–Uranus). The initial conditions of the planets are taken from DE405 ephemerids, and the inner planets have been taken into account by applying a barycentric correction to the initial condition (see Milani and Knežević 1992). The integrator used is a four order symplectic integrator described in Guzzo 2001, specifically designed for the symplectic integration of the outer Solar System. All integrations have been done with integration step 0.2 yr, except for figure 2 top–left which has been done for control with integration step 0.05 yr. The smallest step gives accurate results for our purposes: only errors of at most $10^{-8} - 10^{-7}$ rad/yr are introduced on the secular frequencies of the planets (see Guzzo 2001). Of course, the computation of figure 2 top–right and bottom is affected by larger errors, but the

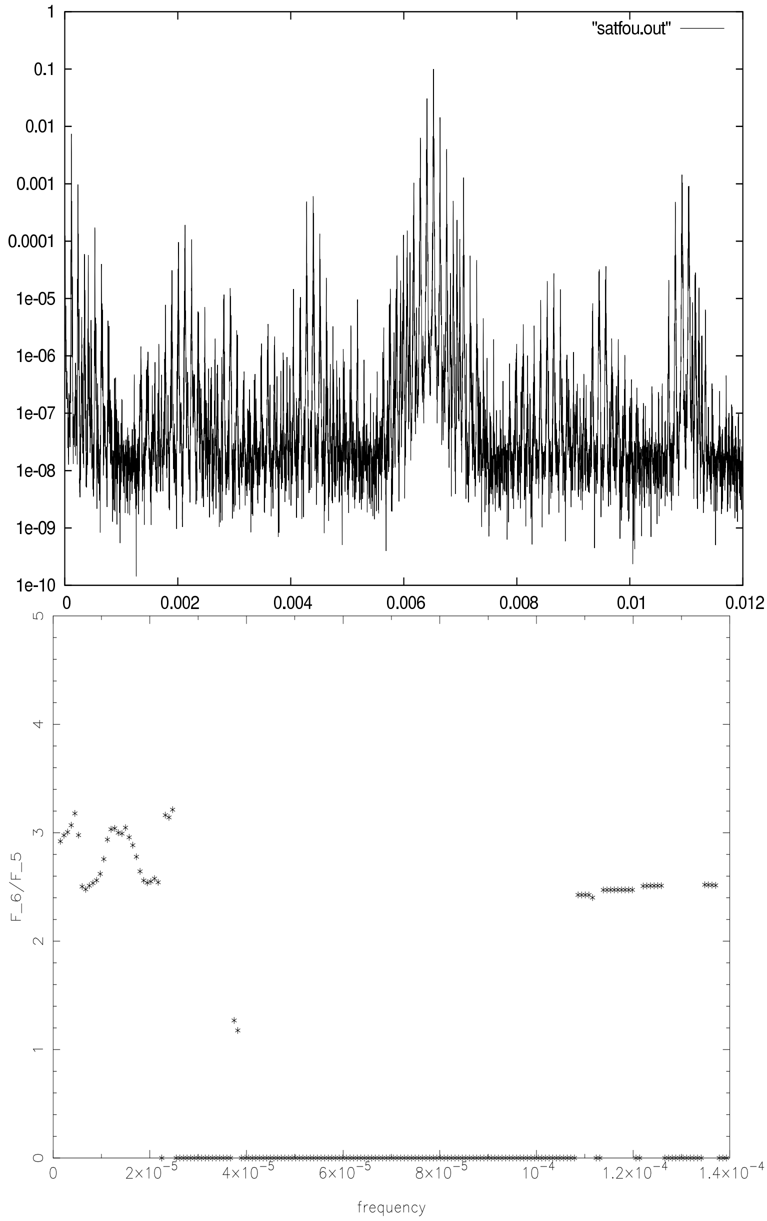

Figure 4: Top: Spectrum of $\phi(t)(L_6(t) - L_6(0))$, related to the motion of Saturn. The three families of quasi–resonances $(2, -5, 0, 0)$, $(0, 1, -3, 0)$ and $(2, -6, 3, 0)$ generate the multiplets located around the frequencies $6.51 \cdot 10^{-3}$, $1.102 \cdot 10^{-2}$ and $4.3 \cdot 10^{-3}$. Bottom: ratio $y_\sigma = F^6_\sigma / F^5_\sigma$ versus frequency σ; if the value of F^6_σ or F^5_σ is too small (10^{-7} in the plot) we set $y_\sigma = 0$.

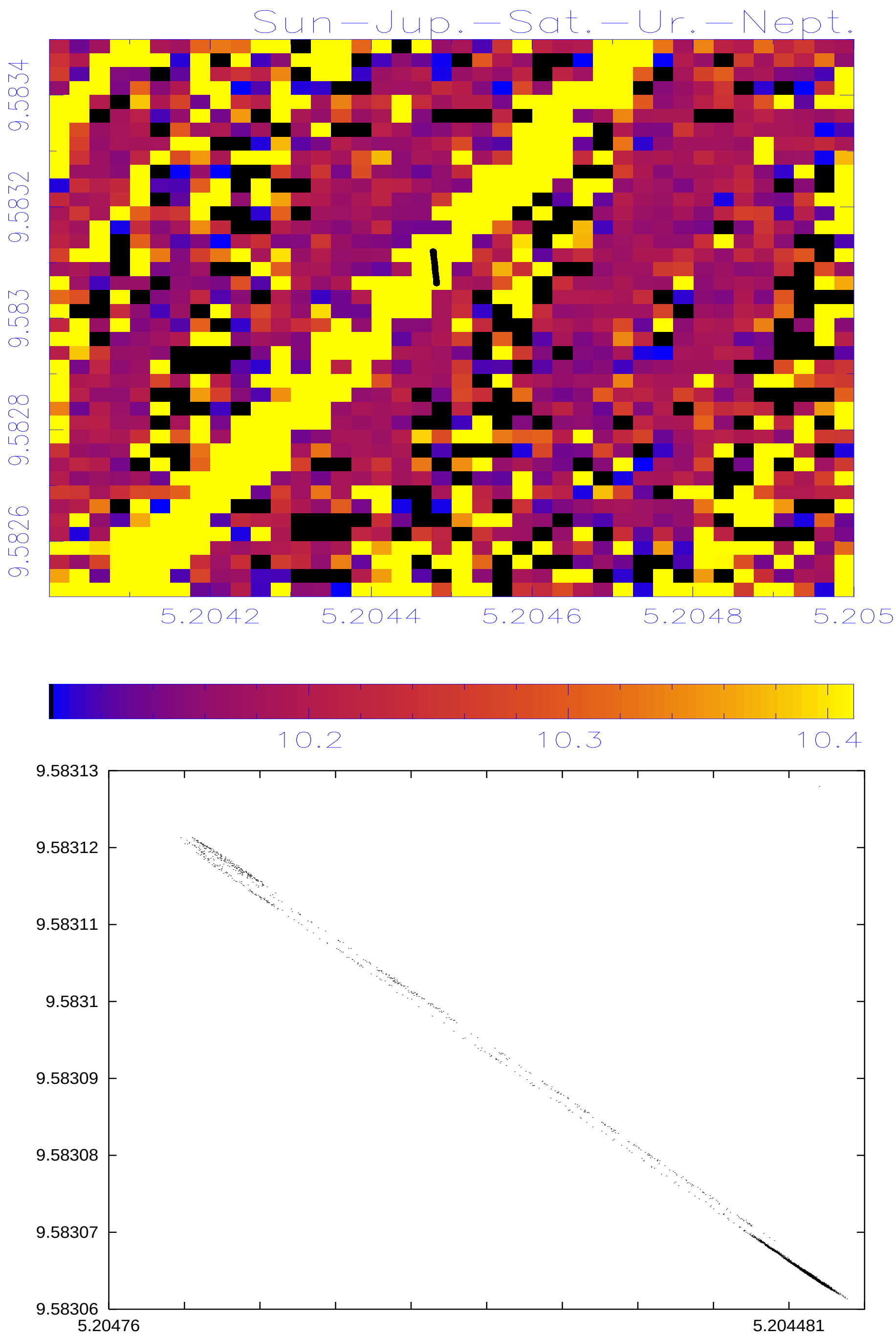

Figure 5: Diffusion of a test initial condition in the resonance $n_6/n_5 = 3$. On both pictures we print the averaged semi–major axes of Saturn and Jupiter each 2 Myr of the orbit integrated up to 3 Gyr. On the top the orbit is represented on the FLI map of the three–body resonances (the x, y axis of the picture reports the initial values of the semi–major axes of Jupiter and Saturn). On this picture we appreciate that the main variation of the orbit is along a direction which is transverse to the resonance. On the bottom we represent a zoom of the orbit which allows one to appreciate also a much smaller (and much slower) variation of the orbit of about $1.4\ 10^{-6}$ au in the direction which is aligned with the resonance. This variation occurs in the interval of time $[5\ 10^8, 7\ 10^8]$ yr, and therefore has an average speed of $7\ 10^{-15}$ au/yr. Precisely, denoting with $a_5(t), a_6(t)$ the values of the semi major axes of the numerically computed orbit and with $\tilde{a_5}(2\ k\ 10^6), \tilde{a_6}(2\ k\ 10^6)$ the averaged semi–major axis in the interval $t \in [2\ k\ 10^6, 2\ (k+1)\ 10^6]$, we print a dot corresponding to: $\tilde{a_5}(2\ k\ 10^6) + d_5, \tilde{a_6}(2\ k\ 10^6) + d_6$, where $d_5 = \tilde{a_5}(0) - a_5(0), d_6 = \tilde{a_5}(0) - a_5(0)$. The average over 2 Myr is done to minimize all projection effects, while the adjustment of (d_5, d_6) is necessary in order to represent the averaged values on the grid of initial osculating semi–major axes.

comparison with figure 2 top–left shows that these errors do not affect the location of the three–planet resonances. The larger integration step allowed us to refine the grid of initial conditions and to extend the integration time from 10^7 yr to 2.10^7 yr. The symplectic method used has also the advantage that, being implemented as a simple map on the heliocentric canonical variables position–momentum, it allows one to simply write the variational equations which are necessary to compute the evolution of tangent vectors, and therefore of the FLI.

The FLI indicator (Freschlé et al. 1997) is the logarithm of the norm of a tangent vector taken at the end of the computation, with the same initial tangent vector for any initial condition on the grid. A detailed description of the method has been already given in section 2.

The frequency analysis used to produce figure 2 is based on Laskar's method (see, for example, Laskar 1993). Precisely, we computed the frequencies of the mean anomalies of Jupiter and Saturn using a Fourier analysis on the time interval $t \in [t_0, t_0 + 10^4]yr$. Of course, if one computes the frequencies on different times intervals $t \in [t_0, t_0 + 10^4]yr$ one obtains different values. However, because the main variation of the computed frequencies with respect to the initial time t_0 is a quasi–periodic oscillation, for the purpose of using these values to represent the geometry of resonances it is sufficient to keep the same $t_0 = 0$ for all initial conditions of the grid.

References

Bretagnon, P. 1981. Construction d'une theorie des grosses planetes par une methode iterative. Astron. & Astrophys. 101, 342–349.

Bretagnon, P. 1982. Theorie du mouvement de l'ensamble des planetes. Solution VSOP82. Astron. & Astrophys. 114, 278–288.

Froeschle' C., Guzzo, M. and Lega, E. 2000. Graphical Evolution of the Arnold Web: From Order to Chaos. Science, 289, 2108–2110.

Froeschlé, C., Lega, E. and Gonczi, R. 1997. Fast Lyapunov Indicators. Application to asteroidal motion. Celest. Mech. and Dynam. Astron. 67, 41–62.

Guzzo, M. 2001. Improved Leap-Frog Symplectic Integrators for Orbits of Small Eccentricity in the Perturbed Kepler Problem. Celest. Mech. and Dynam. Astron. 80, 63-80.

Guzzo, M. 2002. Long–term stability analysis of quasi–integrable degenerate systems through the spectral formulation of the Nekhoroshev theorem. Celest. Mech. and Dynam. Astron. 83, 303–323.

Guzzo, M., Lega, E. and Froeschlé, C. 2002. On the numerical detection of the effective stability of chaotic motions in quasi-integrable systems. Physica D 163, 1-25.

Guzzo, M. and Benettin, G. 2001. A spectral formulation of the Nekhoroshev theorem and its relevance for numerical and experimental data analysis. Discrete and Continuous Dynamical Systems-Series B 1, 1–28.

Guzzo, M. and Morbidelli, A. 1997. Construction of a Nekhoroshev like result for the asteroid belt dynamical system. Celest. Mech. Dyn. Astron. 66, 255–292.

Laskar, J. 1989. A numerical experiment on the chaotic behaviour of the solar system. Nature 338, 237–238.

Laskar, J. 1990. The chaotic motion of the solar system - A numerical estimate of the size of the chaotic zones. Icarus 88, 266–291.

Laskar, J. 1993. Frequency analysis of a dynamical system. Celest. Mech. Dyn. Astron. 56, 191–196.

Laskar, J. 1996. Marginal stability and chaos in the solar system (Lecture). In: Ferraz–Mello, S., Morando, B., Arlod, J. (Eds.), Dynamics, ephemerides, and astrometry of the solar system: proceedings of the 172nd Symposium of the International astronomical Union, held in Paris, France, 38 July, 1995, 75–88.

Laskar, J. 2003. Chaos in the Solar System. Ann. Henri Poincaré 4, Suppl. 2, 693–705.

Locatelli, U. and Giorgilli, A. 2000. Invariant Tori in the Secular Motions of the Three-body Planetary Systems. Celest. Mech. Dyn. Astron. 78, 47–74.

Milani, A. and Knežević, Z. 1992. Asteroid proper elements and secular resonances. Icarus 98, 211–232.

Mitchenko, T.A. and Ferraz–Mello, S. 2001a. Resonant structure of the outer solar system in the neighbourhood of the planets. A.J. 122, 474–481.

Mitchenko, T.A. and Ferraz–Mello, S. 2001b. Modeling the 5:2 Mean-Motion Resonance in the Jupiter-Saturn Planetary System. Icarus 149, 357–374.

Morbidelli, A. 2002. Modern Celestial Mechanics. Aspects of Solar System Dynamics. Taylor and Francis.

Morbidelli, A. and Guzzo, M. 1997. The Nekhoroshev theorem and the asteroid belt dynamical system. Celest. Mech. Dyn. Astron. 65, 107–136.

Morbidelli, A. and Nesvorny, D. 1999. Numerous weak resonances drive asteroids towards terrestrial planets orbits. Icarus 139, 295–308.

Murray, N., Holman, M. and Potter, M. 1998. On the origin of chaos in the solar system. Astron. J. 116, 2583–2589.

Murray, N. and Holman, M. 1999. The origin of chaos in the Outer Solar System. Science 283, 1877–1881.

Nesvorny, D. and Morbidelli, A. 1998a. Three–body mean motion resonances and the chaotic structure of the asteroid belt. Astron. J. 116, 3029–3037.

Nesvorny, D. and Morbidelli, A. 1998b. An analytic model of three–body mean motion resonances. Celest. Mech. and Dyn. Astr. 71, 243–271.

Nobili, A.M., Milani, A. and Carpino, M. 1989. Fundamental frequencies and small divisors in the orbits of the outer planets. Astron. Astrophys., 210, 313–336.

Robutel P. 2004. Frequency map analysis and quasiperiodicdecompositions, In "Hamiltonian systems and Fourier analysis", Editor: Benest et al., Taylor& Francis, in press.

Robutel, P. and Laskar, J. 2001. Global dynamics in the Solar System. Proc. of the US/European Celestial Mechanics Workshop, Poznan, 3–7 July 2000. Kluwer Academic Publishers, Dordrecht, 253–258.

Sussman, G.J. and Wisdom, J. 1988. Numerical evidence that the motion of Pluto is chaotic. Science 241, 433–437.

Sussman, G.J. and Wisdom, J. 1992. Chaotic evolution of the Solar System. Science 257, 56–62.